Magnetic ordering in terbium ethyl sulphate

M. T. Hirvonen, T. E. Katila, K. J. Riski, and M. A. Teplov*
Low Temperature Laboratory, and Department of Technical Physics, Helsinki University of Technology, SF-02150 Otaniemi, Finland

B. Z. Malkin
Kazan State University, 420008 Kazan, United Soviet Socialist Republic

N. E. Phillips and Marilyn Wun†
Inorganic Materials Research Division of the Lawrence Berkeley Laboratory and Department of Chemistry, University of California, Berkeley, California 94720

(Received 27 January 1975)

The magnetic properties of terbium ethyl sulphate, a singlet crystal-field ground-state system with predominantly dipolar interactions between the magnetic ions, have been studied theoretically and experimentally at low temperatures. The susceptibilities parallel and perpendicular to the hexagonal c axis were measured in the temperature range 0.03–4 K by a superconducting-quantum-interference-device magnetometer in connection with a dilution refrigerator. In addition, the heat capacity of a powdered sample was measured. The results indicate a cooperative transition at 0.24 K. The data give indirect information on the value of the crystal-field splitting, which has not been measured before. The behavior of the longitudinal susceptibility is consistent with a picture of a ferromagnetic transition into long and thin domains along the c axis. The much smaller transverse susceptibility shows an unexpected abrupt change at 0.24 K. Theoretical calculations on the magnetic properties are presented. The molecular-field approximation, two- and three-particle "cluster" models and high-temperature expansion are considered in turn. The predictions of the three-particle cluster model are closest to the experimental data.

I. INTRODUCTION

Magnetic ordering in rare-earth compounds has long been subject to intensive experimental and theoretical investigation. The interaction of the orbital angular momentum with the crystal electric field may be comparable to the interionic coupling. If the rare-earth ion has an odd number of $4f$ electrons, the crystal-field energy levels will be at least twofold degenerate. In this case, an ordered state can always be reached by sufficiently lowering the temperature. On the other hand, for a non-Kramers ion the crystal-field ground state is often a singlet, for which the matrix elements of the components of the magnetic moment vanish. In this case the interionic coupling must exceed a critical value relative to the crystal-field splitting in order to have magnetic ordering even at absolute zero.[1,2] The crystal-field effects, which tend to oppose the ordering, become stronger as the orbital contribution to the total angular momentum of the magnetic ion increases. Accordingly, the ordering temperature in general decreases on going from the center of the rare-earth series towards either end. The ordering occurs via magnetic moments which are self-consistently induced by the interactions between the magnetic ions.

Most of the work done on singlet-ground-state magnetism has dealt with systems where exchange interactions are responsible for the ordering.[3,4] One such system, $Tm_2(SO_4)_3 \cdot 8H_2O$, was studied earlier in our laboratories by heat-capacity measurements with powdered samples.[5] However, incomplete knowledge of the crystal structure and the interactions between the magnetic ions made it difficult to carry out detailed comparisons between theory and experiment.

Magnetic ordering in materials with strong dipole-dipole interactions has also been studied.[6-9] However, those investigations deal with cases where the crystal-field ground state is a Kramers doublet. In view of this it is of interest to study magnetic ordering in a system of two crystal-field singlets, with dipole-dipole couplings as the dominant part of the interactions responsible for the ordering. Such a situation prevails in terbium ethyl sulphate (TbES). The crystal structure of the rare-earth ethyl sulphates is well known.[10] The arrangement of the rare-earth ions in the lattice is shown in Fig. 1. The shortest distance between rare-earth ions is along the c direction and equal to about 7 Å.[11] The $^7F_6$ ground state of the Tb^{3+} is split by the crystal field in a rare-earth ethyl sulphate so that the two lowest-energy levels are singlets. The level separation Δ of the Tb^{3+} ion dilute in yttrium ethyl sulphate was determined by paramagnetic resonance measure-

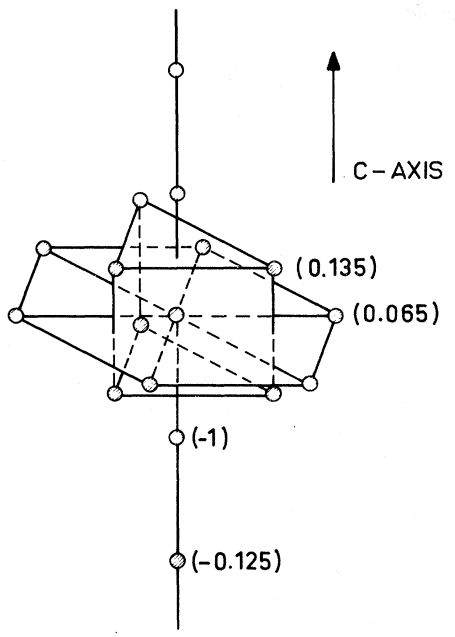

FIG. 1. Arrangement of the magnetic ions in the rare-earth ethyl sulphate lattice. The numbers in parentheses indicate the relative strengths of the magnetic dipole-dipole interaction with the central ion when both spins are oriented parallel to the c axis. The unit of energy is the nearest-neighbor interaction energy, equal to about 0.28 K.

ments to be 0.56 K.[12] The other crystal-field levels lie high enough to be negligible at liquid-helium temperatures. The nearest-neighbor dipole-dipole interaction energy is approximately 0.28 K. Besides, the components of the g tensor and the hyperfine coupling constant have been determined by EPR to be[13] $g_{\parallel} = 17.82 \pm 0.05$, $g_{\perp} = 0$, and $A = 0.303 \pm 0.003$ K. The coupling of the electron spin to the nuclear spin is thus even stronger than the interionic coupling. A NMR study[14] of TbES indicated no magnetic ordering down to 0.33 K.

A study of the magnetic properties of TbES at low temperatures has been carried out. Measurements of magnetic susceptibility and specific heat of single crystal and powder samples are reported in Sec. II. In Sec. III some calculations concerning the magnetic transition are presented. The experimental and theoretical results are discussed in Sec. IV.

II. EXPERIMENTAL INVESTIGATIONS

A. Magnetic susceptibility

Susceptibility measurements on TbES in the temperature region 0.03–4 K were carried out with a superconducting quantum interference device (SQUID) magnetometer in connection with a dilution refrigerator. The magnetometer consists essentially of a superconducting flux transformer inductively coupled to a SQUID.[15] A transformer coil is wound around the tail of the mixing chamber, inside which the specimen is located. The tail is surrounded by a superconducting cylinder, and the flux trapped in the cylinder can be varied from run to run by introducing an external field prior to the superconducting transition. The quantity actually measured is the feedback voltage of the SQUID magnetometer. Changes in this voltage are proportional to changes in the static magnetization of the sample. The initial setting of the feedback voltage is arbitrary, and this inherent uncertainty in the zero of the scale is an obvious drawback. However, if Curie's law applies at the high-temperature end of our measurement range, which seems to be the case, extrapolation will yield the zero of the scale. Another disadvantage is the limited sensitivity of our magnetometer at large susceptibilities.

A calibration run with CMN, whose susceptibility is known as a function of temperature, was needed to obtain the conversion of the measured voltage values to susceptibility values. The same run served as a calibration of the carbon and germanium resistors used for temperature measurement. To simplify the susceptibility calibration it is desirable to use the same shape and size for the CMN sample and the specimen under study. We chose a cylinder whose diameter and height were equal to about 3 mm, because for a CMN powder sample of such a form the shape correction is very small.[16] Besides, such a sample is easy to cut from a single crystal and to orient in the desired manner.

In Fig. 2 the susceptibility per unit density of

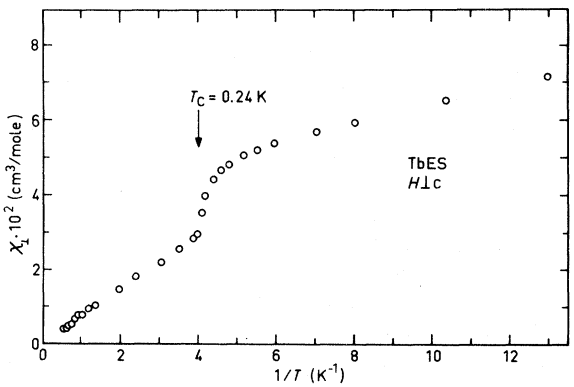

FIG. 2. Transverse molar susceptibility of TbES vs inverse temperature, measured with a SQUID magnetometer. The trapped field was 4.5 G. The arrow indicates approximately the point where the direction of curvature changes.

TbES measured with the field perpendicular to the hexagonal c axis ($\chi_\perp$) is plotted as a function of inverse temperature. The abrupt change in the vicinity of 0.24 K marks a transition to a magnetically ordered state, which is obvious also from the specific-heat curve shown later (Fig. 4).

The measured longitudinal susceptibility $\chi_\parallel$ (field parallel to the c axis) of TbES is shown in Fig. 3. As expected, the signal is much stronger than in the transverse direction, the difference being about three orders of magnitude. The behavior of $\chi_\parallel$ is rather smooth, and at 0.24 K it is already essentially saturated. At the lowest end of our measurement range (below about 0.13 K) it was necessary to wait for a long time, even for some hours at each temperature in order to reach equilibrium.

B. Specific heat

The total heat capacity of a powdered sample of TbES was measured in the temperature region 0.15–20 K. The TbES powder was mixed with Apiezon N grease to make thermal contact to a finned copper sample holder. The heat capacities of the grease and the sample holder were determined in separate experiments. The measurements from the lowest temperatures to 0.6 K were done in an adiabatic demagnetization cryostat using a germanium resistance thermometer that had been calibrated against single-crystal CMN. Measurements were carried out from 0.3 to 20 K in a ^{3}He cryostat using a germanium resistor calibrated against CMN and ^{4}He vapor pressure. As in the measurement of the longitudinal susceptibility, long thermal relaxation times were encountered below 0.18 K, and they increased with further decreases in temperature. By 0.12 K the time constant had increased to about $\frac{1}{2}$ h, and reliable data could not be obtained at lower temperatures.

The measured heat capacity is shown in Fig. 4. There is a very sharp drop with increasing T at 0.24 K, indicating a second-order cooperative transition. Between 2 and 4 K the data fit the formula $C = 1.791T^{-2} + 0.006\,49T^3$ J/mole K, and this was used as a basis for separation of the magnetic and lattice heat capacities. The T^3 term represents the low-temperature lattice heat capacity C_L, which is negligible below 1 K. The curve has no other maximum than the transition peak, but there seems to be a broad Schottky-like anomaly centered at about 0.3 K, which corresponds to a crystal-field splitting of approximately 0.6 K. Below about 0.16 K the specific heat increases again, but unfortunately a reliable determination was not possible in that region.

III. THEORETICAL CONSIDERATIONS

In order to compare the measured magnetic properties of TbES with theoretical estimates we present in the following some calculations concerning the transition temperature and the behavior of the susceptibility and of the specific heat. Similar calculations for dysprosium ethyl sulphate (DyES) have been carried out by Cooke *et al.*[7]

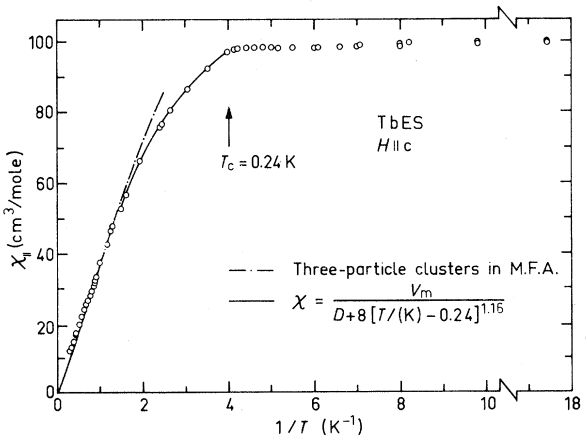

FIG. 3. Longitudinal susceptibility of TbES vs inverse temperature, measured with the Earth's field trapped. The solid curve is a plot of the modified MFA expression (7), and the dashed curve is the result of a three-particle-cluster calculation [Eq. (33)]. V_m is the molar volume of TbES, =357 cm^3.

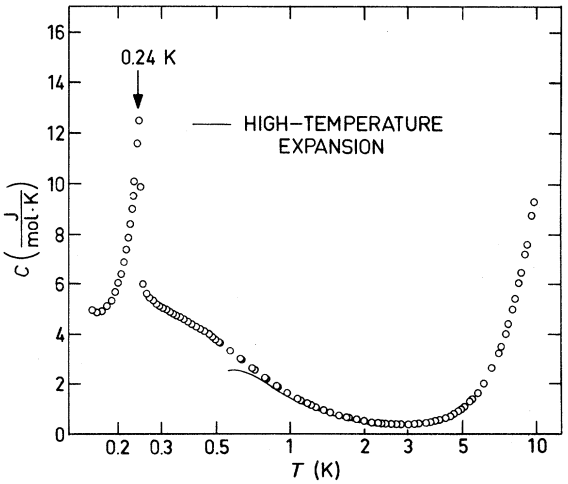

FIG. 4. Heat capacity of powdered TbES as a function of temperature. The temperature scale is logarithmic. The solid curve is the plot of a fourth-order high-temperature expansion (39).

A. Molecular-field approximation

At temperatures where only the two lowest crystal-field levels are populated the appropriate effective spin Hamiltonian for TbES in terms of the Pauli spin operators σ_{ix}, σ_{iz} is

$$\mathcal{H} = \frac{1}{2}\sum_i (g\mu_B \boldsymbol{H}_z \sigma_{iz} + \Delta\sigma_{ix}) + \frac{1}{2}\sum_{ij} I_{ij}\sigma_{iz}\sigma_{jz} + \mathcal{H}_{\rm hf}, \quad (1)$$

where

$$I_{ij} = \tfrac{1}{4} g^2 \mu_B{}^2 \frac{r_{ij}{}^2 - 3z_{ij}{}^2}{r_{ij}^5} \quad (2)$$

is the magnetic dipole-dipole coupling factor, and

$$\mathcal{H}_{\rm hf} = \sum_i \left[\tfrac{1}{2} A\sigma_{iz} I_{iz} + P(3I_{iz}^2 - \tfrac{15}{4})\right], \quad (3)$$

where the nuclear spin $I = \frac{3}{2}$. The nuclear Zeeman interaction has been omitted. The magnitude of the quadrupole interaction is not likely to correspond to more than a few mK, as can be estimated from the value (158 MHz) in DyES.[17] Therefore, the quadrupole term will be neglected in the following.

In the molecular-field approximation (MFA) the interaction term in (1) is simplified by replacing one of the σ's by $\langle\sigma_z\rangle$. The remaining lattice sum depends on the shape of the sample, and it is customary to perform the summation in parts. For zero external field and vanishing hyperfine interaction the resulting Hamiltonian is

$$\mathcal{H}_{\rm MFA} = \frac{1}{2}\sum_i \Delta\sigma_{ix} - k\lambda(p + \tfrac{4}{3}\pi - D)\langle\sigma_z\rangle \sum_i \sigma_{iz}, \quad (4)$$

where

$$\lambda = \frac{(g\mu_B)^2}{4k}\frac{N}{V} = 0.0833 \text{ K} \quad (5)$$

is the Curie constant for $S = \frac{1}{2}$ (in cgs units), and N/V is the particle density. The first contribution p to the second term in (4) comes from the ions within a sphere centered on the ion considered. The contribution from the ions outside the sphere is usually calculated in the continuum approximation and it consists of two terms, $\frac{4}{3}\pi$ corresponding to the Lorentz field, and $-D$ corresponding to the demagnetizing field. The demagnetization factor D has a rigorous meaning only for an ellipsoidal specimen.

The second term in (4) can be interpreted as a molecular field

$$H_M = \tfrac{1}{2} g\mu_B (p + \tfrac{4}{3}\pi - D)\langle\sigma_z\rangle N/V = (p + \tfrac{4}{3}\pi - D)M \quad (6)$$

acting on any one ion. It is proportional to the magnetization $M = \frac{1}{2} g\mu_B \langle\sigma_z\rangle N/V$, hence the measured susceptibility obtained from Curie's law is

$$\chi = \frac{M}{H_z} = \frac{\lambda}{T - \lambda(p + \frac{4}{3}\pi - D)}. \quad (7)$$

For a long and thin specimen, $D = 0$ when the external field is parallel to the long axis. If we assume that at the transition a domain structure sets in, which consists entirely of long and thin domains, then for $\Delta = 0$ the transition temperature within each domain and therefore of the whole sample would be

$$T_c = \lambda(p + \tfrac{4}{3}\pi), \quad (8)$$

independent of the shape of the sample. Accordingly, the behavior of the sample would be described by

$$\chi = \frac{\lambda}{T - T_c + \lambda D}. \quad (9)$$

Naturally, this is only a crude approximation, and a closer fit to the experimental points can be obtained with the modified expression

$$\frac{1}{\chi} = D + B\left(\frac{T - T_c}{K}\right)^{\gamma}, \quad (10)$$

which was used in the analysis of susceptibility measurements of some rare-earth hydroxides.[18] Using $T_c = 0.24$ K, the best fit to our experimental value is obtained for $D = 3.6$, $B = 8$, and $\gamma = 1.16$ (see Fig. 3). The parameter γ deviates less from the MFA value ($\gamma = 1$) than in $Tb(OH)_3$, where $\gamma = 1.26$. This may be expected, since short-range exchange interactions are absent in TbES, while they dominate in $Tb(OH)_3$.

If the hyperfine term is left out from the Hamiltonian (1), then in the MFA for $D = 0$ the transition temperature is given by the equation[19]

$$\tanh\frac{\Delta}{2kT_c} = \frac{\Delta}{2\lambda(p + \frac{4}{3}\pi)} = \frac{1}{\delta}. \quad (11)$$

The molecular-field constant p was calculated by Cooke *et al.*[7] to be = 4.21 for DyES. Using this value and $\Delta = 0.63$ K, as estimated from our specific-heat measurements (see Sec. IIID), we obtain $T_c(\text{MFA}) = 0.649$ K. The inclusion of the hyperfine interaction leads to a more complex equation for T_c,

$$\frac{2\lambda(p + \frac{4}{3}\pi)}{\sum_{m=-3/2}^{3/2} \cosh\epsilon_m/2kT_c} \times \sum_{m=-3/2}^{3/2}\left[\frac{\Delta^2}{\epsilon_m^3}\sinh\frac{\epsilon_m}{2kT_c} + \frac{A^2m^2}{2kT_c\epsilon_m^2}\cosh\frac{\epsilon_m}{2kT_c}\right] = 1, \quad (12)$$

$$\epsilon_m = (\Delta^2 + A^2 m^2)^{1/2} .$$

However, only a small change in T_c results, $T_c(\mathrm{MFA, HF}) = 0.651$ K. It is seen that the MFA overestimates the critical temperature, as noted earlier by Felsteiner and Friedman.[9] The reason for this is that the MFA does not adequately represent the interactions, which are much stronger along the c axis than perpendicular to it (see Fig. 1).

We next consider the specific heat. Taking the expectation value of the MFA Hamiltonian (4) we obtain the energy of the system,

$$E = \tfrac{1}{2} N\Delta\langle\sigma_x\rangle - \tfrac{1}{4} N\Delta\delta\langle\sigma_z\rangle^2 . \tag{13}$$

In the ferromagnetic region $\langle\sigma_z\rangle$ is given by the equation

$$\tanh\frac{\epsilon}{kT} = \frac{2\epsilon}{\delta\Delta}, \quad \epsilon = \tfrac{1}{2}\Delta(1 + \delta^2\langle\sigma_z\rangle^2)^{1/2} . \tag{14}$$

Hence,

$$E = \frac{N}{2}\left(\frac{\Delta^2}{4\epsilon} - \epsilon\right)\tanh\frac{\epsilon}{kT} \tag{15}$$

and

$$C = \frac{dE}{dT} = Nk\left(\frac{\epsilon}{kT}\right)^2 \frac{1}{\cosh^2\epsilon/kT}\left(1 - \frac{\Delta\delta}{2kT\cosh^2\epsilon/kT}\right)^{-1} . \tag{16}$$

In the paramagnetic region $\langle\sigma_z\rangle = 0$ and the specific heat is given by the usual Schottky expression

$$C = Nk\left(\frac{\Delta}{2kT}\right)^2 \frac{1}{\cosh^2\Delta/2kT} . \tag{17}$$

The magnitude of the jump in the specific heat at the critical temperature [given by (11)] is

$$\Delta C(T_c) = Nk\left(\frac{\Delta}{2kT_c}\right)^2 \frac{1}{\cosh^2\Delta/2kT_c} \times \frac{(\delta^2-1)\ln[(\delta+1)/(\delta-1)]}{2\delta - (\delta^2-1)\ln[(\delta+1)/(\delta-1)]} . \tag{18}$$

The numerical value is $\Delta C(T_c) = 9.1$ J/mole K. The maximum value of the heat capacity given by (16) is 10.8 J/mole K. The corresponding experimental value is 12.5 J/mole K.

B. Two-particle cluster

It is clear from Fig. 1 that TbES is essentially a system of rather loosely coupled Ising chains in the direction of the c axis. Therefore, it is to be expected that a model which treats some intrachain interactions rigorously and other interactions by the MFA will yield better results than the above MFA values. Such an approach was successfully used by Cooke *et al.*[7] to improve the agreement between measured and calculated susceptibility values of DyES. The simplest case is that of a "cluster" of two adjacent ions (subscripts 1 and 2) in a chain, for which the Hamiltonian is easily obtained from (1) (we again neglect the hyperfine interactions),

$$\mathcal{H}^{(2)} = -I\sigma_{1z}\sigma_{2z} + \tfrac{1}{2}\Delta(\sigma_{1x} + \sigma_{2x}) + \tfrac{1}{2} g\mu_B(H_z + H_M')(\sigma_{1z} + \sigma_{2z}) , \tag{19}$$

where

$$I = (g\mu_B)^2/2c^3 = 0.283 \text{ K} ,$$

where c is the interionic distance along the c axis, equal to 7.04 Å (DyES), H_M' is the molecular field due to all ions except the other member of the cluster. For our model to be consistent, the average value of the magnetic moment of either ion in the cluster divided by the volume V per ion must be equal to the intensity of magnetization. Hence, we can write, as in (6),

$$H_M' = \frac{g\mu_B\langle\sigma_{iz}\rangle}{2V}(p' + \tfrac{4}{3}\pi - D) , \tag{20}$$

where p' is obtained by subtracting from p the contribution of the other ion in the cluster, $p' = 4.21 - 3.385 = 0.825$.

To obtain an equation for the critical temperature we write the self-consistency condition for $\langle\sigma_{iz}\rangle$ in terms of the density matrix of the cluster, which depends on $\langle\sigma_{iz}\rangle$,

$$\langle\sigma_{iz}\rangle = \mathrm{Tr}[\sigma_{iz}\rho(\langle\sigma_{iz}\rangle)] . \tag{21}$$

Using perturbation theory to calculate the matrix $\sigma_{iz}\rho$ for $H_z = 0$ and $\langle\sigma_{iz}\rangle \to 0$ we find, for a domain with $D = 0$,

$$\frac{4I\lambda(p' + \frac{4}{3}\pi)}{\Delta^2(\cosh\epsilon_1/kT_c + \cosh\epsilon_3/kT_c)}\left(\cosh\frac{\epsilon_1}{kT_c} - e^{\epsilon_3/kT_c} + \frac{\epsilon_1^2 + \epsilon_3^2}{2\epsilon_1\epsilon_3}\sinh\frac{\epsilon_1}{kT_c}\right) = 1 , \tag{22}$$

where ϵ_1 and ϵ_3 are energy eigenvalues of (19) in the absence of H_z and H'_M, i.e.,

$$\epsilon_{1,2} = \pm (I^2 + \Delta^2)^{1/2}, \quad \epsilon_{3,4} = \pm I \ . \tag{23}$$

The graphical solution of (22) yields $T_c = 0.53$ K, still far from the experimental value.

C. Three-particle cluster

The next model to be considered is a cluster of three consecutive ions. We treat the interaction of the central ion 1 with its nearest neighbors 2 and 3 rigorously, represent the interactions of the ions 2 and 3 with their outer nearest neighbors by a magnetic field h, and other interactions by the MFA. Then the Hamiltonian for the cluster is

$$\mathcal{H}^{(3)} = -I\sigma_{1z}(\sigma_{2z}+\sigma_{3z}) + \tfrac{1}{2}\Delta(\sigma_{1x}+\sigma_{2x}+\sigma_{3x}) + \mathcal{V} \ ,$$
$$\mathcal{V} = \tfrac{1}{2}g\mu_B(H_z+H''_M)(\sigma_{1z}+\sigma_{2z}+\sigma_{3z}) + \tfrac{1}{2}g\mu_B(\sigma_{2z}+\sigma_{3z}) \ . \tag{24}$$

The molecular field H''_M is given by (20) when p' is replaced by $p'' = 4.21 - 2\times 3.385 = -2.56$. The value of the parameter h is determined by the requirement that the ions in the chain are equivalent:

$$\langle\sigma_{1z}\rangle = \langle\sigma_{2z}\rangle = \langle\sigma_{3z}\rangle \ , \tag{25}$$

which gives h in terms of $H_z + H''_M$. The averaging is done within the density matrix $\rho(H_z, h)$ of the cluster.

We treat $\mathcal{V}$ in (24) as a perturbation. To find the unperturbed energy eigenvalues an eighth-order secular equation needs to be solved. If the quantization axis is chosen along the x axis, the equation factorizes as follows:

$$\epsilon \pm \tfrac{1}{2}\Delta = 0 \ ,$$
$$8\epsilon^3 \pm 4\Delta\epsilon^2 - (32I^2 + 10\Delta^2)\epsilon \mp \Delta(16I^2 - 3\Delta^2) = 0 \ . \tag{26}$$

The resulting energy levels are

$$\epsilon_1 = -\epsilon_5 = \tfrac{1}{2}\Delta \ ,$$
$$\epsilon_2 = -\epsilon_6 = \tfrac{1}{6}\Delta + a\cos\tfrac{1}{3}\alpha \ ,$$
$$\epsilon_3 = -\epsilon_7 = \tfrac{1}{6}\Delta + a\cos(\tfrac{1}{3}\alpha + \tfrac{2}{3}\pi) \ , \tag{27}$$
$$\epsilon_4 = -\epsilon_8 = \tfrac{1}{6}\Delta + a\cos(\tfrac{1}{3}\alpha - \tfrac{2}{3}\pi) \ ,$$

where

$$a = (4/\sqrt{3})(I^2 + \tfrac{1}{3}\Delta^2)^{1/2} \ ,$$
$$\cos\alpha = -(16\Delta/3a^3)(I^2 - \tfrac{4}{9}\Delta^2) \ .$$

The numerical values for $\Delta = 0.63$ K are

$$\epsilon_1 = 0.315 \text{ K}, \quad \epsilon_2 = 1.071 \text{ K},$$
$$\epsilon_3 = -0.765 \text{ K}, \quad \epsilon_4 = 0.009 \text{ K} \ .$$

The first-order perturbed wave functions

$$\psi_\alpha^{(1)} = \psi_\alpha^{(0)} + \sum_{\beta\neq\alpha} \frac{\langle\psi_\beta^{(0)}|V|\psi_\alpha^{(0)}\rangle}{\epsilon_\alpha - \epsilon_\beta}\psi_\beta^{(0)} \tag{28}$$

are then used to calculate the average value of $\langle\sigma_{iz}\rangle$,

$$\langle\sigma_{iz}\rangle = \frac{1}{Z}\sum_{\alpha=1}^{8}\langle\psi_\alpha^{(1)}|\sigma_{iz}|\psi_\alpha^{(1)}\rangle e^{-\epsilon_\alpha/kT} \ , \tag{29}$$

where

$$Z = \sum_{\alpha=1}^{8} e^{-\epsilon_\alpha/kT} \ . \tag{30}$$

We note here that the condition $\langle\sigma_{1z}\rangle = \langle\sigma_{2z}\rangle$ gives for h a linear dependence on $H_z + H''_M$ in a form $h = g(T)(H_z + H''_M)$, where $g(0) = 0$. It means that magnetic ordering within one chain is possible only at $T = 0$.

For the small-field susceptibility

$$\chi_0 = \lim_{H\to 0}\frac{\langle M\rangle}{H} = -\frac{g\mu_B}{2V}\left.\frac{d\langle\sigma_{iz}\rangle}{dH}\right|_{H=0} \ , \tag{31}$$

we find, by using (26),

$$\chi = -\frac{g\mu_B}{2V}\left(\frac{\partial\langle\sigma_{2z}\rangle}{\partial h}\frac{\partial\langle\sigma_{1z}\rangle}{\partial H_z} - \frac{\partial\langle\sigma_{1z}\rangle}{\partial h}\frac{\partial\langle\sigma_{2z}\rangle}{\partial H_z}\right) \Big/ \frac{\partial\langle\sigma_{2z}-\sigma_{1z}\rangle}{\partial h} \ , \tag{32}$$

where all derivatives are to be taken at $H_z = 0$. When $\langle\sigma_{1z}\rangle$ and $\langle\sigma_{2z}\rangle$ from (29) are inserted, an expression for the longitudinal paramagnetic susceptibility for a sample of TbES with a demagnetization factor D is obtained:

$$\chi_\parallel = \frac{\chi_0}{1 - \chi_0(p'' + \frac{4}{3}\pi - D)} \ , \tag{33}$$

where

$$\chi_0 = \frac{2\lambda}{Z}\frac{R^2 + QS}{R + Q} \ ,$$
$$R = 3.678\cosh\frac{\epsilon_2}{kT} - 3.344\cosh\frac{\epsilon_3}{kT} - 0.335\cosh\frac{\epsilon_4}{kT} \ ,$$
$$Q = -3.549\sinh\frac{\epsilon_2}{kT} - 2.347\sinh\frac{\epsilon_3}{kT} + 0.771\sinh\frac{\epsilon_4}{kT} \ ,$$
$$S = 3.175\sinh\frac{\epsilon_1}{kT} + 5.286\sinh\frac{\epsilon_2}{kT} + 4.233\sinh\frac{\epsilon_3}{kT} + 66.02\sinh\frac{\epsilon_4}{kT}$$

The critical temperature for a domain with $D=0$ is given by the equation

$$1-\chi_0(p''+\tfrac{4}{3}\pi)=0\ . \tag{34}$$

A graphical solution gives $T_c=0.40$ K.

The longitudinal susceptibility, calculated from (33) for a spherical sample, is plotted in Fig. 3.

D. High-temperature expansion

In general, the magnetic susceptibility of a system with Hamiltonian $\mathcal{H}$ can be expressed in terms of the free energy $F=-kT\ln \mathrm{Tr}e^{-\mathcal{H}/kT}$ as $\chi=-\partial^2F/\partial H^2$. At high temperatures, a truncated series expansion can be used to approximate χ (we use the notation $\tilde{\mathrm{T}}\mathrm{r}\,\mathcal{H}^n=\mathrm{Tr}\,\mathcal{H}^n/\mathrm{Tr}1$),

$$\chi=\frac{1}{2kT}\frac{\partial^2}{\partial H^2}\left(\tilde{\mathrm{T}}\mathrm{r}\,\mathcal{H}^2-\frac{1}{3kT}\tilde{\mathrm{T}}\mathrm{r}\,\mathcal{H}^3+\frac{1}{12(kT)^2}[\tilde{\mathrm{T}}\mathrm{r}\,\mathcal{H}^4-3(\tilde{\mathrm{T}}\mathrm{r}\,\mathcal{H}^2)^2]-\frac{1}{60(kT)^3}[\tilde{\mathrm{T}}\mathrm{r}\,\mathcal{H}^5-10\,\tilde{\mathrm{T}}\mathrm{r}\,\mathcal{H}^2\,\tilde{\mathrm{T}}\mathrm{r}\,\mathcal{H}^3]\right.$$
$$\left.+\frac{1}{360(kT)^4}[\tilde{\mathrm{T}}\mathrm{r}\,\mathcal{H}^6-10(\tilde{\mathrm{T}}\mathrm{r}\,\mathcal{H}^3)^2+30(\tilde{\mathrm{T}}\mathrm{r}\,\mathcal{H}^2)^3-15\,\tilde{\mathrm{T}}\mathrm{r}\,\mathcal{H}^2\,\tilde{\mathrm{T}}\mathrm{r}\,\mathcal{H}^4]\right)\ . \tag{35}$$

The coefficients of the powers of T^{-1} depend on the shape of the sample in a system with dipolar interactions. In this case it is convenient to use an expansion[20,21] for χ^{-1} instead of χ:

$$\chi^{-1}=\frac{T}{\lambda}\left(1-\frac{\theta}{T}+\frac{B_2}{T^2}+\frac{B_3}{T^3}+\frac{B_4}{T^4}+\cdots\right), \tag{36}$$

because, then, only the coefficient θ is shape dependent. The coefficients B_n can be derived by comparing (35) with (36). Neglecting again the hyperfine interactions in the Hamiltonian (1), we obtain

$$\begin{aligned}
\theta&=-\frac{1}{k}\sum_j I_{ij}-(D-\tfrac{4}{3}\pi)\lambda\\
B_2&=\frac{1}{k^2}\left(\sum_j I_{ij}^2+\frac{1}{12}\Delta^2\right)\ ,\\
B_3&=\frac{2}{k^3}\left(\frac{1}{3}\sum_j I_{ij}^3-\sum_{j>k} I_{ij}I_{jk}I_{ki}\right)\ ,\\
B_4&=\frac{1}{k^4}\left(-\frac{2}{3}\sum_j I_{ij}^4-6\sum_{j>k} I_{ij}I_{jk}^2I_{ki}\right.\\
&\quad\left.+2\sum_{j>k>l} I_{ij}I_{jk}I_{kl}I_{li}+\tfrac{11}{720}\Delta^4\right)-\tfrac{17}{60}B_2(\Delta/k)^2\ .
\end{aligned} \tag{37}$$

By using the lattice parameters of DyES and results from Refs. 7 and 8 we can evaluate the coefficients in (37),

$$\theta=0.35\ \mathrm{K},\quad B_2=0.21\ \mathrm{K}^2,$$
$$B_3=-0.0095\ \mathrm{K}^3,\quad B_4=-0.03\ \mathrm{K}^4\ .$$

Because of our superconducting magnetometer, measurements could not be carried out much above 4 K, and this prevents us from accurately determining the initial splitting Δ. Moreover, inspection of the values of the coefficients B_n shows that our third-order expansion (36) begins to lose its accuracy already at about $5T_c$. Also, because the coefficients do not decrease monotonically in magnitude, an attempt to estimate the transition temperature by analyzing the asymptotic behavior of the expansion (36) does not appear meaningful.

The specific-heat curve can also yield information on Δ. For that purpose we calculate a high-temperature expansion for the specific heat,

$$\begin{aligned}
C&=-T\frac{\partial^2F}{\partial T^2}\\
&=\frac{1}{kT^2}\left(\tilde{\mathrm{T}}\mathrm{r}\,\mathcal{H}^2-\frac{1}{kT}\tilde{\mathrm{T}}\mathrm{r}\,\mathcal{H}^3+\frac{1}{2(kT)^2}\tilde{\mathrm{T}}\mathrm{r}\,\mathcal{H}^4\right.\\
&\quad\left.-3(\tilde{\mathrm{T}}\mathrm{r}\,\mathcal{H}^2)^2+\cdots\right).
\end{aligned} \tag{38}$$

By using the Hamiltonian (1) we obtain

$$\frac{C}{R}=\frac{b_2}{(kT)^2}+\frac{b_3}{(kT)^3}+\frac{b_4}{(kT)^4}\ , \tag{39}$$

where

$$\begin{aligned}
b_2&=\tfrac{1}{4}(g\mu_BH_z)^2+\tfrac{1}{4}\Delta^2+\frac{1}{2}\sum_j I_{ij}^2+\tfrac{5}{16}A^2\ ,\\
b_3&=-\tfrac{3}{4}(g\mu_BH_z)^2\sum_j I_{ij}-2\sum_{j>k} I_{ij}I_{jk}I_{ki}\ ,\\
b_4&=-\tfrac{1}{8}(g\mu_BH_z\Delta)^2+3(g\mu_BH_z)^2\sum_{j>k} I_{ij}I_{ik}-\tfrac{1}{16}\Delta^4\\
&\quad-\tfrac{1}{2}\Delta^2\sum_j I_{ij}^2-\frac{1}{2}\sum_j I_{ij}^4+3\sum_{j>k>l} I_{ij}I_{jk}I_{kl}I_{li}\\
&\quad-\tfrac{5}{32}\Delta^2A^2-\tfrac{17}{256}A^4\ .
\end{aligned}$$

For $H_z=0$ and $\Delta=0.56$ K,[12] the numerical values of the coefficients are

$$b_2=0.195\ \mathrm{K}^2,\quad b_3=0.0176\ \mathrm{K}^3,\quad b_4=-0.0412\ \mathrm{K}^4\ .$$

The solid curve in Fig. 4 is a plot of the sum of (39) for these values of the coefficients and the

lattice heat capacity. It does not agree well with the experimental points. By adjusting the parameter Δ, of which b_2 and b_4 are functions, to give the best agreement with the experimental points between 1.5 and 4 K, an estimate of 0.63 K for Δ is obtained.

IV. DISCUSSION

A. Transition temperature

The transition temperatures given by the transverse susceptibility (Fig. 2) and the specific heat (Fig. 4) are in good agreement with each other. Our calculation of T_c within the different models yielded results which consistently exceed the experimental value 0.24 K, but show a trend towards it as the models become more realistic. The results of the calculations depend on the value of the initial splitting Δ, for which we have used the value 0.63 K extracted from our specific-heat data on the basis of a fourth-order high-temperature expansion. However, given the slow convergence of the expansion, this value can hardly be considered reliable. The real splitting in TbES can be even greater than 0.63 K, and this is a possible reason for the discrepancy between the calculated and experimental values of T_c.

B. Specific heat

The analysis of our specific-heat data is complicated by the strength of the hyperfine interaction relative to the crystal-field splitting. In fact, the transition should be thought of as that of a compound electron-nucleus system. This is reflected in the behavior of the entropy, which we obtain by separating the lattice contribution to the specific heat. The entropy decrease from $T=\infty$ to $T=0.24$ K is already $1.03R\ln 2$; to $T=0.20$ K, just below the sharp peak, it is $1.37R\ln 2$. Clearly the nuclear-spin entropy begins to decrease already above 0.24 K.

Because our experimental specific-heat data show no maximum above T_c, the molecular-field calculation for zero hyperfine interaction, which yields a pure Schottky curve above T_c, cannot be made to agree with the measurements. Since the MFA does not yield the correct value for T_c, even a more accurate calculation including the hyperfine interaction is not expected to result in a curve which agrees with the experimental data. For the same reason we did not calculate the specific heat in the cluster models discussed above. Such calculations are not likely to give additional information on the properties of TbES.

C. Susceptibility

Although EPR measurements have shown that $g_\perp$ is approximately zero, we have observed a finite susceptibility in the transverse direction (Fig. 2). The results shown in Fig. 2 were obtained with a trapped field of 4.5 G. Another measurement in a trapped field of 9 G gave the same slope for the approximately linear part of $\chi_\perp$ both above and below T_c as the measurement with 4.5 G. However, the magnitude of the abrupt change in $\chi_\perp$ at T_c was not the same in these two measurements, nor was it proportional to the trapped field.

According to our estimate the temperature-independent Van Vleck susceptibility, due to the excited electronic states of the Tb^{3+} ion, is approximately 3×10^{-2} cm^3/mole in TbES. This value is of the same order of magnitude as the transverse susceptibility. However, because the SQUID magnetometer used in the measurements only indicates changes in magnetization, the Van Vleck contribution is presumably not included in our experimental data.

Misalignment of the sample is a possible source of error in the transverse susceptibility. If the c axis is not exactly perpendicular to the trapped field, the longitudinal susceptibility will contribute to the measured value of $\chi_\perp$. However, this would only happen in a region where $\chi_\parallel$ varies with temperature, and therefore cannot account for the behavior of $\chi_\perp$ at and below T_c.

Another possible source of error is the presence of paramagnetic impurity ions, such as Gd^{3+} or Er^{3+}. Their contribution to $\chi_\perp$ would be linear in T^{-1}. The amount of, e.g., Er^{3+} ions needed to account for the slope of $\chi_\perp$ below T_c is about 0.03 at.%. The presence of such small amounts of impurities in our specimens cannot be ruled out. We therefore consider, if a jump like the one observed in $\chi_\perp$ at T_c could be caused by paramagnetic impurities.

Above T_c the magnetic moment per unit volume due to the impurities is

$$M_\perp(T>T_c)=\chi_i H \ , \tag{41}$$

where χ_i is the susceptibility of the impurities (assumed isotropic) and H is the trapped field. Below T_c the sample is made up of long and thin domains along the c axis. A strong molecular field H_M, parallel to the c axis, appears within these domains. If the trapped field were exactly perpendicular to the c axis, H_M would give no contribution to the magnetization along H. On the other hand, if H makes an angle θ with the c axis, then the magnetization due to the impurities below T_c is

$$\begin{aligned} M_\perp^+ &= \chi_i(H+H_M\cos\theta) \text{ for } + \text{ domains}, \\ M_\perp^- &= \chi_i(H-H_M\cos\theta) \text{ for } - \text{ domains} . \end{aligned} \tag{42}$$

The magnetization of the sample as a whole is then

$$M_\perp(T<T_c) = aM_\perp^+ + (1-a)\,M_\perp^- , \tag{43}$$

where a is the fraction of + domains. At T_c there is a jump in the magnetization,

$$\Delta M_\perp = M_\perp(T<T_c) - M_\perp(T>T_c)$$
$$= (2a-1)\,\chi_i H_M \cos\theta . \tag{44}$$

On the other hand, the longitudinal magnetization of the sample below T_c is

$$M_\parallel = \chi_\parallel H\cos\theta = (1/D)H\cos\theta = (2a-1)M_0 , \tag{45}$$

where M_0 is the magnetization within the domains. Therefore,

$$\Delta M_\perp = \frac{H_M}{M_0}\,\frac{\cos^2\theta}{D}\,\chi_i H , \tag{46}$$

and because for a long and thin domain[7] $H_M = 8.4M_0$, we obtain finally

$$\Delta\chi_\perp = (8.4\cos^2\theta/D)\,\chi_i . \tag{47}$$

We see that the jump at T_c should be independent of the trapped field and very small for small misalignments (θ close to 90°). Hence it seems unlikely that the observed behavior of $\chi_\perp$ is due to paramagnetic impurities.

After considering some possible sources for the transverse susceptibility in TbES we still lack a satisfactory explanation for it. A study of the transverse susceptibility of TbES single crystals doped with controlled amounts of paramagnetic impurities could be helpful in finding out the possible role of impurities in causing the observed results.

V. CONCLUSION

(i) A ferromagnetic ordering has been observed in TbES at 0.24 K. The transition is most clearly indicated by the specific heat.

(ii) The temperature dependence of the longitudinal susceptibility of TbES agrees with calculations based on a model of long and thin domains along the c axis of the crystal.

(iii) Among the models considered, the three-particle cluster combined with the molecular-field approximation gives the best agreement with experimental results for the transition temperature and the longitudinal susceptibility in the paramagnetic region.

(iv) An anomalous temperature dependence of the transverse susceptibility of TbES has been observed.

---

*Present address: Kazan State University, Kazan, United Soviet Socialist Republic.
†Present address: Department of Chemistry, University of California, Los Angeles, Calif. 90024.

[1]B. Bleaney, Proc. R. Soc. A 276, 19 (1963).
[2]G. T. Trammell, Phys. Rev. 131, 932 (1963).
[3]Y-L. Wang and B. R. Cooper, Phys. Rev. 172, 539 (1968).
[4]Y-L. Wang and B. R. Cooper, Phys. Rev. 185, 696 (1969).
[5]T. E. Katila, N. E. Phillips, M. C. Veuro, and B. B. Triplett, Phys. Rev. B 6, 1827 (1972).
[6]J. H. Van Vleck, J. Chem. Phys. 5, 320 (1937).
[7]A. H. Cooke, D. T. Edmonds, C. B. P. Finn, and W. P. Wolf, Proc. R. Soc. A 306, 313 (1968); A 306, 335 (1968).
[8]E. Lagendijk, H. W. J. Blöte, and W. J. Huiskamp, Physica (Utr.) 61, 220 (1972).
[9]J. Felsteiner and Z. Friedman, Phys. Rev. B 7, 1078 (1973).
[10]D. R. Fitzwater and R. E. Rundle, Z. Krystallogr. 112, 362 (1959).
[11]R. J. Anderson, J. M. Baker, and R. J. Birgeneau, J. Phys. C 4, 1618 (1971).
[12]J. M. Baker and B. Bleaney, Proc. R. Soc. A 245, 156 (1958).
[13]A. R. King, Bull. Am. Phys. Soc. 13, 434 (1968).
[14]S. A. Al'tshuler, F. L. Aukhadejev, I. I. Valejev, I. S. Konov, B. Z. Malkin, and M. A. Teplov, Zh. Eksp. Teor. Fiz. Pis'ma Red. 16, 233 (1972) [JETP Lett. 16, 164 (1972)].
[15]R. P. Giffard, R. A. Webb, and J. C. Wheatley, J. Low Temp. Phys. 6, 533 (1972).
[16]R. P. Hudson, Cryogenics 9, 76 (1969).
[17]S. Hüfner, H. H. Wickman, and C. F. Wagner, Phys. Rev. 169, 247 (1968).
[18]W. P. Wolf, H. Meissner, and C. A. Catanese, J. Appl. Phys. 39, 1134 (1968).
[19]R. Bidaux, A. Gavignet-Tillard, and J. Hamman, J. Phys. 34, 19 (1973).
[20]J. M. Daniels, Proc. Phys. Soc. Lond. A 66, 673 (1953).
[21]W. P. Wolf, B. Schneider, D. P. Landau, and B. E. Keen, Phys. Rev. B 5, 4472 (1972).